Interactions between cardiac, respiratory, and EEG-δ oscillations in rats during anæsthesia

Bojan Musizza,[1,2] Aneta Stefanovska,[*3,2] Peter V. E. McClintock,[3] Milan Paluš,[4]
Janko Petrovčič,[1] Samo Ribarič[5] & Fajko F. Bajrović[5,6]

[1]Department of Systems and Control, Jožef Stefan Institute, Jamova 39, Ljubljana, Slovenia
[2]Nonlinear Dynamics and Synergetics Group, Faculty of Electrical Engineering,
University of Ljubljana, Tržaška 25, Ljubljana, Slovenia
[3]Department of Physics, Lancaster University, Lancaster LA1 4YB, UK
[4]Institute of Computer Science, Academy of Sciences of the Czech Republic,
Pod vodárenskou věží 2, 182 07 Prague 8, Czech Republic
[5]Institute of Pathophysiology, Faculty of Medicine, University of Ljubljana,
Zaloška 7, Ljubljana, Slovenia
[6]Department of Neurology, Clinical Centre Ljubljana, Zaloška 7, Ljubljana, Slovenia

*To whom correspondence should be addressed.

Communications data for correspondence

Address: Dr Aneta Stefanovska,
Department of Physics,
Lancaster University,
LA1 4YB Lancaster, United Kindom.

E-mail: aneta@lancaster.ac.uk

Tel: + 44 1524 592784

Fax: + 44 1524 844037

Abstract

We hypothesised that, associated with the state of anæsthesia, there exist characteristic changes in both cardio-respiratory and cerebral oscillator parameters and couplings, perhaps varying with depth of anaesthesia. Electrocardiograms (ECGs), respiration and electroencephalograms (EEGs) were recorded from two groups of 10 rats during the entire course of anæsthesia following the administration of a single bolus of ketamine-xylazine (KX group) or pentobarbital (PB group). The phase dynamics approach was then used to extract the instantaneous frequencies of heart beat, respiration and slow δ-waves (within 0.5–3.5 Hz). The amplitudes of δ- and θ-waves were analysed by use of a time-frequency representation of the EEG signal within 0.5–7.5 Hz obtained by wavelet transformation, using the Morlet mother wavelet. For the KX group, where slow δ-waves constituted the dominant spectral component, the Hilbert transform was applied to obtain the instantaneous δ-frequency. The θ-activity was spread over too wide a spectral range for its phase meaningfully to be defined.

For both agents, we observed two distinct phases of anæsthesia, with a marked increase in θ-wave activity occurring on passage from a deeper phase of anæsthesia to a shallower one. In other respects, the effects of the two anæsthetics were very different. For KX anæsthesia, the two phases were separated by a marked change in all three instantaneous frequencies: stable, deep, anæsthesia with small frequency variability was followed by a sharp transition to shallow anæsthesia with large frequency variability, lasting until the animal awoke. The transition occurred 16–76 minutes after injection of the anæsthetic, with simultaneous reduction in the δ-wave amplitude. For PB anæsthesia, the two epochs were separated by the return of a positive response to the pinch test at 53–94 minutes, following which it took a further period of 45–70 minutes for the animal to awaken. δ-waves were not apparent at any stage of PB anæsthesia.

We applied nonlinear dynamics and information theory to seek evidence of causal relationships between the cardiac, respiratory and slow δ-oscillations. We demonstrate that, for both groups, respiration drives the cardiac oscillator during deep anæsthesia. During shallow KX anæsthesia the direction either reverses, or the cardio-respiratory interaction becomes insignificant; in the deep phase, there is a unidirectional deterministic interaction of respiration with slow δ-oscillations. For PB anæsthesia, the cardio-respiratory interaction weakens during the second phase but, otherwise, there is no observable change in the interactions. We conclude that nonlinear dynamics and information theory can be used to identify different stages of anæsthesia and the effects of different anæsthetics.

Cardiac and respiratory oscillations have long been known to interact with each other, the resultant respiratory modulation of cardiac frequency, respiratory sinus arrythmia, having first been observed in the eighteenth century (Hales 1773). Synchronisation of the cardiac and respiratory oscillations provides another manifestation of their interaction. Several recent studies have demonstrated the existence of such synchronisation (Pikovsky *et al.* 2001), which was shown to be stronger in young athletes (Schäfer *et al.* 1998) than in young healthy non-athletes (Lotrič & Stefanovska 2000). However, the precise physiological basis of the cardio-respiratory interaction is still emerging (Eckberg 2003). Galletly & Larsen (1997) have shown that the cardio-respiratory interaction is changed during anæsthesia. It was further demonstrated by application of the phase dynamics approach that phase-transition-like phenomena in synchronisation occur sequentially in rats as their anæsthesia is made deeper or lighter (Stefanovska *et al.* 2000), paving the way to an improved understanding of the physiology of anæsthesia.

Studies of neuronal oscillations have been undertaken since the first human electroencephalographic (EEG) recordings by Berger (1929). The recent resurgence of interest in such oscillations has led to an enhanced appreciation of their likely importance and to the tantalising conjecture that perception, memory and even consciousness could result from the synchronisation of neuronal networks (Buzsáki & Draguhn 2004). Anæsthesia is another state where neuronal oscillations synchronise and desynchronise. Based on a large number of studies, John (2002) and John & Prichep (2005) have proposed a neurophysiolgical theory of the action of anæsthetics in suppressing awareness. They distinguish six steps leading to decreased γ-coherence and increased frontal δ- and θ-oscillations as a result of the depression of the prefrontal cortex reducing awareness.

We hypothesised that interactions occur between cardio-respiratory and neuronal oscillations. To test this idea, we have applied stochastic nonlinear dynamics techniques (Pikovsky *et al.* 2001; Stefanovska & Bračič 1999) to the analysis of time-varying physiological oscillations recorded from rats under anæsthesia. The agents chosen were ketamine-xylazine (KX) and pentobarbital (PB), which are commonly used (Destexhe *et al.* 2003; Rudolph & Antkowiak 2004) in neuroscience research. The cardiac and respiratory oscillations were extracted from ECG and respiration signals (Stefanovska & Bračič 1999; McClintock & Stefanovska 2002). The time evolutions of individual neuronal oscillations were extracted from the EEG by means of the wavelet transform (Bračič & Stefanovska 1998; Le Van Quyen *et al.* 2001; Harrop *et al.* 2002), with particular attention being paid to δ- and θ-waves. The instantaneous frequency of δ-oscillations was traced during the deep phase of KX anæsthesia when they were strongly pronounced (see below). The analyses were based on the phase dynamics technique introduced by Kuramoto

(1984) and its subsequent applications to synchronisation analysis (Tass *et al.* 1998; Schäfer *et al.* 1998; Lotrič & Stefanovska 2000; Glass 2001; Pikovsky *et al.* 2001) and to the detection of causal relationships among coupled oscillators (Schreiber 2000; Paluš *et al.* 2001*a*; Paluš & Stefanovska 2003; Rosenblum & Pikovsky 2001; Rosenblum *et al.* 2002). The phase dynamics approach is a particularly useful tool for the investigation of physiological oscillations because it can cope with their time-variable nature, and because it allows us to study their amplitudes and phases separately. It can reveal the underlying rules that contribute to the deterministic part of the variability, thus yielding evidence about its physiological origins. It also illuminates the question of whether there exist causal relationships between the oscillations, and whether some or all of the time variability results from a unidirectional interaction.

We further hypothesised that cardio-respiratory-neuronal interactions would be detectable through causality analyses; and that the oscillation amplitudes, and the strength and directionality of the coupling, would undergo characteristic changes according to depth of anæsthesia and would be specific for each of the anæsthetics used.

METHODS

Experimental procedure

The experiments were performed on two groups of adult, male Wistar rats weighing 250–300 g. Ten animals in the first group were anæsthetized with a single intraperitoneal injection of ketamine hydrocholride (45 mg/kg b.w.) and xylazine hydrochloride (7 mg/kg b.w.) (KX group). Ten animals in the second group were anæsthatised with a single intraperitoneal bolus of pentobarbital (150 mg/kg b.w.) (PB group). As soon as the rat could no longer hold its upright posture (10-15 minutees after administration of the drug), it was placed in a darkened Faraday cage where sensors were mounted and recording started immediately. The experiments took place in the Institute of Pathophysiology in Ljubljana in accordance with: State Guidelines for granting Licenses for Animal Experiments for Research Purposes, published in the *Official Gazette of the Republic of Slovenia* 40/85, 22/87; the Protection of Animals Act, *ibid* 98/99; EU regulations and recommendations, Council Directive 86/609/EEC; European Parliament resolution 2001/2259(INI); and the European Science Foundation Policy Briefing *Use of Animals in Research*, August 2001, Second Edition.

In both groups, simultaneous recordings were made of: EEG over the left and right parietal cortex; electrical activity of the heart (ECG); and respiration. Three hypodermic needles, which served as EEG electrodes, were inserted under the animal's scalp. The EEG was differentially amplified ($A = 10000$) and filtered (low-pass filter $f_c = 300$ Hz). The ECG was measured

differentially ($A = 20$) with three electrodes placed on the animal's tail and front paws. Respiration was monitored by recording chest wall movement using a piezoelectric probe attached over the animal's thorax. All three signals were then fed through a signal conditioning system (CardioSignals, developed by the Jožef Stefan Institute and the Faculty of Electical Engineering, Ljubljana, Slovenia). They were each digitized at 1 kHz with 16-bit resolution (using a National Instruments multifunction I/O data acquisition board) and stored on the hard disk of a laptop computer.

Depth of anæsthesia was assessed at 5 min intervals by a nociceptive stimulus, the skin pinch-test, applied to the sole of the animal's front paw (Bajrović & Sketelj 1998). The recording started with a negative test response, i.e. when the rat stopped responding with a reflex withdrawal of the limb.

In the KX group, monitoring was terminated on the reappearance of a positive pinch-test response, as the animal immediately started to move thereby terminating reliable data recording. The duration of recording varied from rat to rat (see Table 1) and was on average 87 min. Monitoring of the PB group continued for a limited period after the reappearance of a positive pinch-test, while the rat was still not fully awake. It was stopped 45-70 minutes after the reappearance of the positive pinch-test, thus allowing for recording during an interval of the waking state. Again, the duration of recording varied from rat to rat and was on average 92 min.

All measurements were at constant room temperature (24±1)°C. At the end of the recordings the animals were killed by administration of an overdose of the same anæsthetic.

Signal preprocessing

To reduce the effects of noise and artifacts, the recorded signals were preprocessed prior to analysis. The ECG and respiratory signals were bandpass-filtered in the 4–6 and 1–2 Hz intervals respectively (the characteristic frequencies in rats being ∼4 times higher than in humans), with care taken to avoid any introduction of phase lags. The EEG signal was also bandpass-filtered, but only after extensive investigation of its time-frequency content by wavelet analysis. Short samples of time series after pre-processing are shown in Fig. 1.

Wavelet transform

The EEG power spectrum is conventionally divided (John 2002) into the frequency bands: δ (0.5–3.5 Hz); θ (3.5–7.5 Hz); α (7.5–12.5 Hz); β (12.5–25 Hz); γ_1 (25–35 Hz); γ_2 (35–50 Hz); and γ_3 (50–100 Hz). We calculated the time evolution within each band by application of the continuous wavelet transform (Stefanovska & Bračič 1999). Wavelet analysis overcomes an

inherent problem of the windowed Fourier transform for which time and frequency resolution cannot be optimal for all frequencies. It uses a window function of variable width – the mother wavelet $\psi(u)$ – which is shifted in time so that a family of generally non–orthogonal basis functions

$$\Psi_{s,t} = |s|^{-p}\psi\Big(\frac{u-t}{s}\Big) \tag{1}$$

is obtained. Here s is the scale of the wavelet and t is the shift in time; p is an arbitrary non-negative number (usually set to 0.5). The wavelet transform of a signal $g(t)$ is defined as

$$G(s,t) = \int_{-\infty}^{\infty} \Psi_{s,t}(u) g(u)\, du\ . \tag{2}$$

The Morlet mother wavelet was used because it allows direct connection between scale and frequency. To accelerate computation, the signal was first downsampled to 40 Hz. The wavelet transform was then segmented into the conventional EEG frequency intervals (see above).

Fig. 2 shows typical time-frequency plots for the two groups. For the KX group activity occurred mainly in the 0.5–3.5 Hz and 3.5–7.5 Hz bands, in agreement with earlier work (Amzica & Steriade 1998). For the PB group activity was observed only within 3.5–7.5 Hz, and only during the second part of the experiment. For further analysis each signal was divided into two intervals, (i) before and (ii) after the transition. The latter was defined by the diminution of the δ-band signal for the KX group, and by the appearance of θ-activity for the PB group, which usually coincided with the first positive pinch-test. The time for each rat is given in Table 1.

Quantitative analysis of wavelet transform

Values of average wavelet amplitudes, as previously defined for the blood flow signal (Bračič & Stefanovska 1998)

$$A = \frac{1}{\Delta f \Delta t} \int_{t_1}^{t_2} \int_{s_1}^{s_2} s^{-2} |g(s,t)| \mathrm{d}t \mathrm{d}s, \tag{3}$$

were compared statistically for the δ- and θ-band separately for the first and second parts of the recording by use of the Matlab (MathWorks Inc., Natick, Massachusetts, USA) Statistical Toolbox. The data are presented in each case as a boxplot of the paired group differences, thus providing a graphical representation of the data distribution, with box lines at the lower quartile, median, and upper quartile values. The spread of the data is shown by lines extending from each end of the box. A paired Wilcoxon signed rank statistical test was used to test the hypothesis that the differences between the matched samples come from a distribution whose median is zero; $p \leq 0.05$ was considered as statistically significant.

Instantaneous phases

In estimating an instantaneous phase we suppose that the studied processes, $\{X(t)\}$ and $\{Y(t)\}$, can be modelled by weakly-coupled oscillators (Linkens *et al.* 1982; Stefanovska & Bračič 1999) and that their interactions can be inferred by analysis of the dynamics of their instantaneous phases (Kuramoto 1984), $\phi_1(t)$ and $\phi_2(t)$, confined within $[0, 2\pi)$ or $[-\pi, \pi)$. The latter can be estimated from the measured time series $\{x(t)\}$ and $\{y(t)\}$, e.g. by the marked events method, or by application of the discrete Hilbert transform (Pikovsky *et al.* 2001), or by wavelet transform (Bračič & Stefanovska 1998; Le Van Quyen *et al.* 2001; Harrop *et al.* 2002; Quiroga *et al.* 2002).

The instantaneous frequencies of the cardiac (i.e. HRV) and respiratory oscillations were obtained by the marked events method, $f(t) = \frac{1}{t_{k+1}-t_k}$ where t_k and t_{k+1} are the times of consecutive peaks. The instantaneous phases $\phi(t) = 2\pi\frac{t-t_k}{t_{k+1}-t_k} + 2\pi k$, $t_k \leq t < t_{k+1}$ were then obtained, linearly interpolated, and resampled with $\Delta t = 0.05$ s. To obtain the instantaneous frequency corresponding to the δ-oscillations in the EEG, an analytic signal $\zeta(t)$ was constructed from the original time series. This is a complex function of time defined as $\zeta(t) = s(t) + \imath s_H = A(t)e^{\imath\phi(t)}$, where $A(t)$ is the amplitude and $\phi(t)$ is the phase of the signal $s(t)$, and $s_H(t)$ is its Hilbert transform. The instantaneous phase is given by $\phi(t) = \arctan\frac{s_H(t)}{s(t)}$. For comparison we also computed the phases using the complex continuous Morlet wavelet (Torrence & Compo 1998) for the scale 0.64, which gave a period of 0.66 s, i.e. a main central frequency of 1.5 Hz. The instantaneous phase $\phi(t)$ of the cortical δ-oscillations was then found by substitution of the real and imaginary parts of the wavelet coefficient for those of the analytic signal.

We had hoped to extract the instantaneous phases of cardiac, respiratory, δ- and θ-oscillations for both groups. In the event, only the phases of the cardiac and respiratory oscillations could be determined reliably throughout the anæsthesia. The instantaneous phase of the δ-oscillations could be calculated only for the KX group, and then only during the first section of the recording; in the second section, their amplitude became too small. The phase of δ-oscillations for the PB group was undetectable throughout. Note in Fig. 2 that, for most rats in the PB group, a sharp peak (with associated harmonics) appears at the frequency where δ-waves are to be expected in the EEG. However, a very strong coherence (near unity) was found with the instantaneous phase of respiration, showing that the peak is attributable to movement artefacts.

For both groups, the amplitude of θ-oscillations was significant only during the second part of the recordings. Under both anæsthetics, they spanned a large frequency interval (see Fig. 2) so that the notion of an instantaneous phase could not be defined unambiguously. Fig. 3 shows examples of cardiac, respiratory and δ instantaneous phases for one rat during KX (left) and PB (right) anæsthesia. We now explain in detail how the interactions were evaluated.

Detection of interactions among coupled oscillators

We inferred the directionality of coupling using two independent methods, based on: (i) phase dynamics (Rosenblum & Pikovsky 2001; Rosenblum *et al.* 2002); and (ii) information theory (Paluš *et al.* 2001*a*; Paluš & Stefanovska 2003). For studying the coupling and its asymmetry in more detail, we use method (ii). Generally, the mutual information $I(X;Y)$ of two random variables X and Y is given as $I(X;Y) = H(X) + H(Y) - H(X,Y)$. Here the entropies $H(X)$, $H(Y)$, $H(X,Y)$ are given in the usual Shannonian sense (Cover & Thomas 1991; Paluš *et al.* 2001*a*). The entropy and information are usually measured in bits if logarithm to base 2 is used; here we use the natural logarithm for which they are in nats. The conditional mutual information $I(X;Y|Z)$ of the variables X, Y given the variable Z is then defined using the conditional entropies (Cover & Thomas 1991; Paluš *et al.* 2001*a*) as

$$I(X;Y|Z) = H(X|Z) + H(Y|Z) - H(X,Y|Z). \tag{4}$$

Consider two time series $\{x(t)\}$ and $\{y(t)\}$ regarded as realizations of two stationary ergodic stochastic processes $\{X(t)\}$ and $\{Y(t)\}$ representing observables of two possibly coupled systems. Dependence structures between the two processes (time series) can be studied using the simple mutual information $I(y;x_\tau)$, where we use y for $y(t)$ and x_τ for $x(t+\tau)$. $I(y;x_\tau)$ measures the average amount of information contained in the process $\{Y\}$ about the process $\{X\}$ in the future, τ time units ahead (referred to hereafter as the τ-*future*). Note that, if processes $\{X\}$ and $\{Y\}$ are not independent, i.e. if $I(x;y) > 0$, this measure could also contain information about the τ-future of the process $\{X\}$ contained in this process itself; so also could other dependence and predictability measures.

Causal relationships

For inferring causal relationships, i.e. the directionality of coupling between the processes $\{X(t)\}$ and $\{Y(t)\}$, we need to estimate the "net" information about the τ-future of the process $\{X\}$ contained in the process $\{Y\}$ using an appropriate tool – the *conditional mutual information* (CMI) $I(y;x_\tau|x)$. It has been shown (Paluš *et al.* 2001*a*,*b*) that, using $I(y;x_\tau|x)$ and $I(x;y_\tau|y)$, the coupling directionality can be inferred from time series measured in coupled, but not yet fully synchronized systems.

Now suppose that the processes $\{X\}$ and $\{Y\}$ can be modelled by weakly-coupled oscillators and that their interactions can be inferred by analysis of the dynamics of their instantaneous phases $\phi_1(t)$ and $\phi_2(t)$ (Rosenblum & Pikovsky 2001; Rosenblum *et al.* 2002), as stated above. Rather than simply replacing the series $\{x(t)\}$ and $\{y(t)\}$ with the phases $\phi_1(t)$ and $\phi_2(t)$ (which

are confined within the interval $[0, 2\pi)$ or $[-\pi, \pi)$), we consider phase increments

$$\Delta_\tau \phi_{1,2} = \phi_{1,2}(t + \tau) - \phi_{1,2}(t),$$

and the CMI $I(\phi_1(t); \Delta_\tau \phi_2 | \phi_2(t))$ and $I(\phi_2(t); \Delta_\tau \phi_1 | \phi_1(t))$ or, in a shorter notation, $I(\phi_1; \Delta_\tau \phi_2 | \phi_2)$ and $I(\phi_2; \Delta_\tau \phi_1 | \phi_1)$. Next, in analogy with Rosenblum et al. (Rosenblum & Pikovsky 2001; Rosenblum *et al.* 2002) we define a directionality index

$$d_{(1,2)} = \frac{i(1 \to 2) - i(2 \to 1)}{i(1 \to 2) + i(2 \to 1)}, \tag{5}$$

where the measure $i(1 \to 2)$ of how the system 1 drives the system 2 is either equal to the CMI $I(\phi_1; \Delta_\tau \phi_2 | \phi_2)$ for a chosen time lag τ, or to an average of $I(\phi_1; \Delta_\tau \phi_2 | \phi_2)$ over a selected range of lags τ. In full analogy we define $i(2 \to 1)$ using $I(\phi_2; \Delta_\tau \phi_1 | \phi_1)$; $d_{(1,2)}$ is positive if the driving from system 1 to system 2 prevails, and negative for the opposite case.

Note that, if each observed system were responding separately to an unseen third system, they could exhibit correlations without causal connections. Although we cannot rigorously exclude this possibility, our model studies with three variables show that the CMI, evaluated over a range of time lags, should not be significantly changed by such a third variable influencing the other two variables with different delay times.

Statistical analyses with surrogate data

The reliability of the measures was checked through the use of *surrogate data* (Paluš *et al.* 2006). These are artificially generated time-series that preserve the statistical properties of the original data but are randomized such that any possible coupling is removed (Theiler *et al.* 1992; Schreiber & Schmitz 2000). They were constructed by random permutation of the RR intervals, and of the intervals between respiration and δ-wave maxima; and phases were computed using these randomized intervals as described above. This approach should have destroyed any dependence or causal relationship, if present in the original data, while preserving the basic statistical properties (i.e. distributions of cardiac, respiratory and δ-wave frequencies) of the original data which can be sources of bias and variance in estimation of the CMI. Testing of significance was based on the CMI, which quantifies the coupling in each direction. The CMI itself is more reliable than the directionality index (5) given by the normalized difference of two CMIs. Note that, for establishing the significance of the results, the absolute value of the CMI is irrelevant. Rather, it is its difference from the surrogate range that counts. The reason is that a particular data distribution and frequency content lead to a particular bias, and this bias is also preserved in the surrogate data. Consequently, only values that are significantly greater than those from the surrogate data can be taken as reliable evidence of interaction.

RESULTS

The two phases of anæsthesia were defined under Methods. The effect of each anæsthetic was distinctively different. With KX, the rats were fully awake as soon as the pinch test was positive, and the recording was stopped immediately. With PB, even after the rats started reacting to the pinch test, they were not fully awake and recording remained possible for a further period. Thus, the PB light phase was easy to determine reliably and served as a control. Cardiac and respiratory frequency data for all rats are summarised in Table 2.

Instantaneous frequencies

The δ-wave frequency in the EEG of the KX group increases slightly during the initial deep phase of anæsthesia. It undergoes a dramatic decrease in amplitude at the transition from deep to light anæsthesia. The θ-oscillations also undergo changes at the transition (left and right panels of Fig. 2), with a noticeable increase in the amplitude of the latter. In agreement with the earlier study (Stefanovska *et al.* 2000), the respiration frequency increased and became erratic at the transition, and the cardiac frequency increased (Fig. 3). The instantaneous frequencies of cardiac and respiratory oscillations did not undergo any particular changes during the transition from deep to light PB anæsthesia. The only dramatic change during PB anæsthesia was in the phase dynamics of the θ-oscillations, which was similar to that observed in the KX group.

Time-frequency analysis of EEG

Fig. 4 presents box plots with group median values and distributions of spectral amplitudes within the δ and θ frequency intervals for deep and light KX and PB anaæsthesia. Again, the δ-waves are characteristic of KX deep phase anæsthesia and significantly decrease during the light phase. For PB, their amplitudes are low and do not differ significantly between the two phases of anæsthesia. The θ-waves are similar for both anæsthetics, being weak during the deep phase and increasing significantly as the light phase is entered.

The fact that the δ- and θ-oscillations during KX anæsthesia, and the θ-oscillations during PB anæsthesia, undergo changes at the same moment as those in the cardiac and respiratory oscillations suggests the possibility of mutual interactions.

Interactions and causal relationships

Fig. 5 presents details of the cardio-respiratory interaction during KX (left) and PB (right) anæsthesia: the temporal evolution of the directionality index $d_{r,c}$ is plotted, as determined by the phase dynamics (Rosenblum & Pikovsky 2001; Rosenblum *et al.* 2002) and mutual information (Paluš *et al.* 2001*a*; Paluš & Stefanovska 2003) approaches. Note that the directionality indices in Fig. 5 are calculated using short moving windows to obtain their time evolutions. In

each case the interaction during KX is seen to undergo a marked and sudden change at the transition, at the same time as the onset of erratic respiration (Fig. 3-left) and the pronounced decrease in amplitude of the δ-oscillation (Fig. 2-left). Up to that point, the directionality index is positive, i.e. respiration drives cardiac activity as in the waking state. As the anæsthesia becomes shallow, however, this is no longer true and, if anything, it is then the cardiac rhythm that drives respiration. On the contrary, no significant change in cardio-respiratory interactions can be observed during either phase of PB anæsthesia (Fig. 5-right). The results obtained from these two very different methods are clearly in good qualitative agreement.

Causal relationships checked using surrogate data

The analysis was based on the maximum possible window lengths corresponding to each of the two phases of anæsthesia. This means that possible short episodes of interaction will not be observed, but makes for a more reliable estimate of the average interaction during that phase. We now illustrate the surrogate-testing using as an example the cardio-respiratory interactions in rat No. 9 from the KX group. In this case, the first segment (before the transition) is 0–33 minutes, and the second segment (after the transition) is 43–71 minutes. The surrogate data were constructed from the tested data segment, thus retaining the same frequency distribution. The results are presented in Fig. 6, in which the CMI for the original data is represented by the position of a vertical bar, whereas the range of values given by 2500 realizations of the surrogate data is shown as a 100-bin histogram. If the value of CMI for the original data lies within this distribution, it is considered as statistical significance for accepting the null hypothesis (no coupling). Results are shown for the four different cases, i.e. in each direction, before and after the transition. The statistical tests for all 20 rats are summarised in Table 3.

The results of Fig. 6 confirm those of Fig. 5-left, which were obtained with short time windows. Fig. 6*a* shows strong statistical evidence for respiration driving the heart during deep KX anæsthesia; Figs. 6*b,d* provide evidence that there may be a change between deep and shallow anæsthesia in the $i_{c\to r}$ information transfer under PB, though it is not statistically significant. Fig. 6*c* shows that there is no significant $i_{r\to c}$ information transfer in the shallow phase of anæsthesia under KX.

Fig. 7 summarises schematically the main results of the study, based on all 20 rats analysed. It illustrates the existence of causal relationships between cardiac and respiratory oscillations for both KX (*a,b*) and PB (*c,d*) anæsthetics. The direction of coupling reverses between the deep and shallow phases of KX anæsthesia. With PB, the direction of driving remains from respiration to cardiac activity throughout the recording but weakens after the transition, while

the interaction $i_{c\to r}$ in the opposite direction becomes insignificant in the shallow phase.

For the KX group, interactions with the EEG δ-oscillations in the deep phase of anæsthesia are also summarised. Statistically significant evidence for respiration driving the cortical δ-oscillations is established for half of the rats; for the others, the evidence points in the same direction, but is weaker (not statistically significant). A firm signature of driving in the opposite direction is obtained for only one rat, and $p \leq 0.08$ is obtained for additional two rats (see Table 3). No signature of cardiac-δ interactions is obtained for any of the rats and there is a high probability of there being no driving in either direction.

DISCUSSION

Although the two anæsthetics differ markedly in their effects, they share in common a sudden increase in θ-wave activity as an initial deep phase of anæsthesia gives way to lighter anæsthesia.

For KX, the transition from the first phase of anæsthesia to the second (Table 1) occured at a time of 18–73 minutes after the injection. The first period is characterised by the presence of strong δ-oscillations, only, in the EEG. Both the respiratory and cardiac frequencies remain relatively stable. During the second period, δ-oscillations are markedly decreased, either because the underlying activity has lessened, or because it has become spatially desynchronised. Simultaneously, weak activity appears in the θ (3.5–7.5 Hz) interval. At the same time, the cardiac and respiratory instantaneous frequencies increase significantly and their variability becomes very large. We suggest that this may be attributable to the effects of the ketamine wearing off faster that those of xylazine so that during the second phase only xylazine is active.

For PB, the mean cardiac frequency decreased slightly during the deep phase of anæsthesia, and its variability remained very small during the whole period of measurement. The mean respiratory frequency stayed virtually constant, with almost no variability. Soon after the onset of θ-activity, 53–94 minutes after the onset of anæsthesia, the pinch test became positive, but this did not coincide with movements or righting attempts (Devor & Zalkind 2001). The next 45–70 minutes, until the animal awakened, represent shallow anæsthesia.

For KX the two stages clearly differ in respect of the causal relationships between δ, cardiac, and respiratory oscillations. The cardio-respiratory interaction reverses, with respiration strongly driving the cardiac oscillations during the first period. During the second period, the interaction is much weaker, but is in the opposite direction, with respiration being driven by the cardiac oscillations. We have also demonstrated that the respiratory–δ interaction is probably bidirectional, but further investigation is needed. For PB, the cardio-respiratory interaction during deep anæsthesia is bidirectional, with respiration driving the cardiac oscillator in both phases

of anæsthesia, for all rats. Such causal relationships during anæsthesia have not previously been reported. We now discuss their implications.

The observed evolutions of the δ-oscillations for KX, and of θ-oscillations for both KX and PB, are consistent with the results reviewed and the picture proposed by John (2002) and John & Prichep (2005). They concluded from many studies using several different anæsthetics that δ-oscillations are associated with reduced awareness. Using a time-frequency representation of EEG measurements recorded on dogs, Nayak *et al.* (1994) also demonstrated that the δ and θ frequency bands can be related to depth of anæsthesia. Dossi *et al.* (1992) have demonstrated that the majority of thalamocortical neurons are endowed with electrophysiological properties, allowing them to oscillate at 0.5–4 Hz. Steriade *et al.* (1993) have shown that such oscillations are strongly synchronised during sleep, and desynchronised in the waking state. Rhythmic neuronal activity in the frequency range 0.5–4 Hz is now widely accepted (Rudolph & Antkowiak 2004) as characteristic of stages III and IV of non-rapid-eye-movement sleep (also known as slow-wave sleep). It has been shown (Alkire 1998) that the transition from a sedated to an unconscious state is accompanied by a decrease in cortical glucose metabolism and, at the same time, a reduction in β, α and θ power, whereas δ power is increased indicating increased thalamic activity. Alkire *et al.* (2000) have further proposed that thalamocortical cells, which have been identified as the main generators of cortical δ rhythms, are also involved in producing an anæsthetic-induced δ activity similar to natural sleep.

A significant implication of our results is the possibility of quantifying depth of anæsthesia. During the first stage, of KX anæsthesia, all the elements for loss of awareness discussed by John & Prichep (2005) are fulfilled. Initially, there is an abrupt alteration of the brain state but, as the anæsthetic is metabolised, the changes involved in some of the six steps may be reversed leading to the second stage where δ-oscillations decrease and θ-activity starts to return. This is consistent with the suggestion by John & Prichep (2005) that the three dimensions of anæsthesia – immobility, amnesia, and absence of awareness – are mediated by different regions of the central nervous system. Destexhe *et al.* (2003) have recently reviewed the results of simultaneous intracellular and EEG recording in the waking state and during KX and barbiturate anæsthesia. The fact that we have not observed δ-activity in the PB group is probably attributable to the fact that barbiturates profoundly depress cortical excitability and may well affect thalamocortical cells in a similar way. The fact that we can distinguish deep and shallow phases of anæsthesia for two different agents shows that, although further experiments in animals and humans are needed, the approach presented here can be used to trace the changes that occur during anæsthesia.

A second implication is that there exist causal relationships between cardiac, respiratory

and brain oscillatory processes. These results are consistent with earlier work demonstrating the existence of the cardio-respiratory interaction, but substantially extend it by inferring the *direction* of the interaction and through the inclusion of δ-oscillations. Note that Pomfrett *et al.* (1993) pointed out that significant changes in respiratory sinus arhythmia were associated with changes in the median frequency of the EEG following changes in propofol infusion in humans. A temporal relationship between changes in HRV and EEG activity has also been demonstrated during sleep in both humans (Otzenberger *et al.* 1997; Yang *et al.* 2002) and rats (Yang *et al.* 2003). When recording from the olfactory cortex of rats under similar KX anæsthesia Fontanini *et al.* (2003) and Fontanini & Bower (2005) observed that most of the slow oscillations concentrated in the 0.7-1.5 Hz band. They also discovered higher frequencies during light anæsthesia. The relationship between respiration and EEG was also analysed in detail in these two papers. The interaction of respiration with EEG waves may, however, be quite different in the olfactory cortex, with more respiration-related sensory inputs than in the parietal cortex. The complex interactions between cardiac, respiratory and brain rhythms are important, not only for anæsthesia, but also for cognitive and functional disturbances (John 2002). For example, disorders of autonomic cardiovascular control were detected in patients with epilepsy, even in the absence of abnormal findings during EEG monitoring (Massetani *et al.* 1997). Recent studies have started to elucidate the pathways involved in neurovascular regulation in the brain (Iadecola 2004), including the effect of brainstem catecholamine neurons on respiration (Li & Nattie 2006) and the connection between neuronal activity, neuronal oxydative metabolism and astrocytic glycolisis (Kasischke *et al.* 2004).

A third outcome relates to the possible involvement of glial cells in slow δ-waves. Our analysis of time–frequency spectral content within the classical frequency intervals (John, 2002), revealed nonzero amplitudes within 0.5–3.5 Hz, and 3.5–7.5 Hz (Fig. 2). That in 0.5–3.5 Hz was dominant for KX, especially during deep phase anæsthesia. We note that Amzica & Steriade (1998) identified several oscillations, with distinct mechanisms and sites of origin, within the classical δ-band: a slow (< 1 Hz) cortically generated oscillation, a clock-like thalamic oscillation (1–4 Hz) and a cortical oscillation (1–4 Hz). Using the envelope of the power of the higher frequencies or neuronal spikes, Penttonen & Buzsáki (2003) distinguish several slow oscillatory states in rats and, in particular, two components within the classical δ-band 0.5–1.5 and 1.5–4 Hz, named slow-1 and δ respectively. In the present work, the Hilbert transform was used to determine the instantaneous frequency within the interval 0.5–3.5Hz. The frequency varied with time, but remained between 1 and 2 Hz. We assume that, because we detect the compound activity of the brain, the slow-1 and δ-waves reported by Penttonen & Buzsáki (2003) using highly regional

recordings manifest here as a single oscillatory component. The fact that it interacts with respiratory oscillations for KX (Fig. 7) is of particular interest, given the known activity of glial cells in this frequency range (Amzica & Steriade 1998; Amzica 2002), and their pivotal role as intermediaries between neurons and brain microcirculation (Kasischke *et al.* 2004; Zonta *et al.* 2003). It suggests that causality analyses like those described above have potential for revealing details of glial activity *in vivo* that cannot be evaluated in other ways.

In summary, for both KX and PB we have identified two distinct phases of anæsthesia. With KX there is a sudden change in the directionality of the cardio-respiratory interaction as deep anæsthesia gives way to light anæsthesia. Marked changes in EEG δ and θ waves also occur at the transition. Evidence is reported for interactions between respiratory and δ-oscillations, with the former driving the latter during deep anæsthesia.

The research was supported by ARRS (Slovenia), the CMEYS Programme KONTAKT and the Institutional Research Plan AV0Z10300504 (Czech Republic), the Wellcome Trust, the Leverhulme Trust, and the FP6 EC NEST-Pathfinder projct BRACCIA.

REFERENCES

Alkire MT (1998). Quantitative EEG correlations with brain glucose metabolic rate during anesthesia in volunteers. *Anesthesiology* **89**, 323–333.

Alkire MT, Haier RJ & Fallon JH (2000). Toward a unified theory of narcosis: brain imaging evidence for a thalamocortical switch as the neurophysiologic basis of anesthetic-induced unconsciousness. *Conscious Cogn* **9**, 370–386.

Amzica F (2002). In vivo electrophysiological evidences for cortical neuron-glia interactions during slow (< 1 Hz) and paroxysmal sleep oscillations. *J Physiol (Paris)* **96**, 209–219.

Amzica F & Steriade M (1998). Electrophysiological correlates of sleep delta waves. *Electroenceph and Clinical Neurophysiol* **107**, 69–83.

Bajrović F & Sketelj J (1998). Extent of nociceptive dermatomes in adult rats is not primarily maintained by axonal competition. *Exp Neurol* **150**, 115–121.

Berger H (1929). Ueber das elektroenkephalogramm des menschen. *Arch Psychiatr Nervenkr* **87**, 527–570.

Bračič M & Stefanovska A (1998). Wavelet based analysis of human blood flow dynamics. *Bull Math Biol* **60**, 919–935.

Buzsáki G & Draguhn A (2004). Neuronal oscillations in cortical networks. *Science* **304**, 1926–1929.

Cover T & Thomas J, *Elements of Information Theory*. John Wiley and Sons, New York, NY, 1991.

Destexhe A, Rudolph M & Paré D (2003). The high conductance state of neocortical neurons *in vivo*. *Nature Reviews Neuroscience* **4**, 739–751.

Devor M & Zalkind V (2001). Reversible analgesia, atonia, and loss of consciousness on bilateral intracerebral microinjection of pentobarbita. *Pain* **94**, 101–112.

Dossi RC, Nuñez A & Steriade M (1992). Electrophysiology of a slow (0.5–4 hz) intrinsic oscillation of cat thalamocortical neurons invivo. *J Physiol (Lond)* **447**, 215–234.

Eckberg DL (2003). The human respiratory gate. *J Physiol (Lond)* **548**, 339–352.

Fontanini A & Bower JM (2005). Variable coupling between olfactory system activity and respiration in ketamine-xylazine anesthetized rats. *J Neurophysiol* **93**, 3573–3581.

Fontanini A, Spano P & Bower JM (2003). Ketamine-xylazine-induced slow ($<$ 1.5hz oscillations in the rat piriform (olefactory) cortex are functionally correlated with respiration. *J Neurosci* **23**, 7993–8001.

Galletly DC & Larsen PD (1997). Cardioventilatory coupling during anæsthesia. *Brit J Anæsth* **79**, 35–40.

Glass L (2001). Synchronization and rhythmic processes in physiology. *Nature* **410**, 277–284.

Hales S, *Statistical Essays II, Hæmastatisticks*. Innings Manby, London, 1773.

Harrop JD, Taraskin SN & Elliott SR (2002). Instantaneous frequency and amplitude identification using wavelets: Application to glass structure. *Phys Rev E* **66**, 026703.

Iadecola C (2004). Neurovascular regulation in the normal brain and in alzheimer's disease. *Nat Rev Neurosci* **5**, 347–360.

John ER (2002). The neurophysics of consciousness. *Brain Res Rev* **39**, 1–28.

John ER & Prichep LS (2005). The anesthetic cascade: A theory of how anesthesia suppresses consciousness. *Anesthesiology* **102**, 447–471.

Kasischke KA, Vishwasrao HD, Fisher PJ, Zipfel WR & Webb WW (2004). Neural activity triggers neuronal oxidative metabolism followed by astrocytic glycolysis. *Science* **305**, 99–103.

Kuramoto Y, *Chemical Oscillations, Waves, and Turbulence*. Springer-Verlag, Berlin, 1984.

Le Van Quyen M, Foucher J, Lachaux JP, Rodriguez E, Lutz A, Martinerie J & Varela FJ (2001). Comparison of Hilbert transform and wavelet methods for the analysis of neuronal synchrony. *J Neurosci Methods* **111**, 83–98.

Li AH & Nattie E (2006). Catacholamine neurons in rats modulate sleep, breathing, central chemoreception, and breathing variability. *J Physiol (Lond)* **570**, 385–396.

Linkens DA, Kitney RI & Rompelman O (1982). Raster-scan method for observing physiological entrainment phenomena. *Med & Biol Eng & Comput* **20**, 483–488.

Lotrič MB & Stefanovska A (2000). Synchronization and modulation in the human cardiorespiratory system. *Physica A* **283**, 451–461.

Massetani R, Strata G, Galli R, Gori S, Gneri C, Limbruno U, DiSanto D, Mariani M & Murri L (1997). Alteration of cardiac function in patients with temporal lobe epilepsy: Different roles of eeg-ecg monitoring and spectral analysis of rr variability. *Epilepsia* **38**, 363–369.

McClintock PVE & Stefanovska A (2002). Noise and determinism in cardiovascular dynamics. *Physica A* **314**, 69–76.

Nayak A, Roy RJ & Sharma A (1994). Time-frequency spectral representation of the EEG as an aid in the detection of depth of anesthesia. *Annals of Biomed Engin* **22**, 501–513.

Otzenberger H, Simon C, Gronfier C & Brandenberger G (1997). Temporal relationship between dynamic heart rate variability and electroencephalographic activity during sleep in man. *Neurosci Lett* **229**, 173–176.

Paluš M, Komárek V, Hrnčíř Z & Štěrbová K (2001*a*). Synchronization as adjustment of information rates: Detection from bivariate time series. *Phys Rev E* **63**, 046211.

Paluš M, Komárek V, Procházka Z, Hrnčíř Z & Štěrbová K (2001*b*). Synchronization and information flow in EEG of epileptic patients. *IEEE Eng Med Biol Magazine* **20**, 65–71.

Paluš M, Musizza B & Stefanovska A (2006). Testing for coupling asymmetry using surrogate data. *Chaos and Complexity Lett* in press **http://www.cs.cas.cz/˜mp/papers2/dirsur3pr.pdf**.

Paluš M & Stefanovska A (2003). Direction of coupling from phases of interacting oscillators: An information-theoretic approach. *Phys Rev E* **67**, 055201(R).

Penttonen M & Buzsáki G (2003). Natural logarithmic relationship between brain oscillators. *Thalamus & Related Syst* **2**, 145–152.

Pikovsky A, Rosenblum M & Kurths J, *Synchronization – A Universal Concept in Nonlinear Sciences*. Cambridge University Press, Cambridge, 2001.

Pomfrett CJD, Barrie JR & Healy TEJ (1993). Respiratory sinus arrhythmia – an index of light anesthesia. *Brit J Anæsth* **71**, 212–217.

Quiroga RQ, Kraskov A, Kreuz T & Grassberger P (2002). Performance of different synchronization measures in real data: A case study on electroencephalographic signals. *Phys Rev E* **65**, 041903.

Rosenblum MG, Cimponeriu L, Bezerianos A, Patzak A & Mrowka R (2002). Identification of coupling direction: Application to cardiorespiratory interaction. *Phys Rev E* **65**, 041909.

Rosenblum MG & Pikovsky AS (2001). Detecting direction of coupling in interacting oscillators. *Phys Rev E* **64**, 045202.

Rudolph U & Antkowiak B (2004). Molecular and neuronal substrates for general anæsthetics. *Nature Reviews Neuroscience* **5**, 709–720.

Schäfer C, Rosenblum MG, Kurths J & Abel HH (1998). Heartbeat synchronised with ventilation. *Nature* **392**, 239–240.

Schreiber T (2000). Measuring information transfer. *Phys Rev Lett* **85**, 461–464.

Schreiber T & Schmitz A (2000). Surrogate time series. *Physica D* **142**, 346–382.

Stefanovska A & Bračič M (1999). Physics of the human cardiovascular system. *Contemporary Phys* **40**, 31–55.

Stefanovska A, Haken H, McClintock PVE, Hožič M, Bajrović F & Ribarič S (2000). Reversible transitions between synchronization states of the cardiorespiratory system. *Phys Rev Lett* **85**, 4831–4834.

Steriade M, Nuñez A & Amzica F (1993). A novel slow (< 1Hz) oscillation of neocortical neurons *in vivo*: depolarising and hyperpolarising components. *J Neurosci* **13**, 3252–3265.

Tass P, Rosenblum MG, Weule J, Kurths J, Pikovsky A, Volkmann J, Schnitzler A & Freund HJ (1998). Detection of n:m phase locking from noisy data: Application to magnetoencephalography. *Phys Rev Lett* **81**, 3291–3294.

Theiler J, Eubank S, Longtin A, Galdrikian B & Farmer J (1992). Testing for nonlinearity in time series: the method of surrogate data. *Physica D* **58**, 77–94.

Torrence C & Compo GP (1998). A practical guide to wavelet analysis. *Bull Am Meteorol Soc* **79**, 61–78.

Yang CCH, Lai CW, Lai HY & Kuo TBJ (2002). Relationship between electroencephalogram slow-wave magnitude and heart rate variability during sleep in humans. *Neurosci Lett* **329**, 213–216.

Yang CCH, Shaw FZ, Lai CJ, Lai CW & Kuo TBJ (2003). Relationship between electroencephalogram slow-wave magnitude and heart rate variability during sleep in rats. *Neurosci Lett* **336**, 21–24.

Zonta M, Angulo MC, Gobbo S, Rosengarten B, Hossmann KA, Pozzan T & Carmignoto G (2003). Neuron-to-astrocyte signaling is central to the dynamic control of brain microcirculation. *Nature Neurosci* **6**, 43–50.

Table 1: Anæsthesia data for the 20 rats, summarising the times of characterstic events relative to the initiation of anæsthesia. Ten rats received ketamine-xylazine (KX group) and ten received pentobarbital (PB). In the KX group the recording ended with the first positive pinch test. The time of the transition from deep to shallow anæsthesia was based on the changes in f_r (Fig. 3-left) and on the amplitude of the δ-wave (see Fig. 2-left). The increase in f_r is always clearly defined to within a few seconds. The decrease in amplitude of the δ-wave, although dramatic, cannot be localised precisely in time, so an interval is specified during which the change occured. In the PB group, the transition from deep to shallow anæsthesia was based on the pinch test and the time at which the θ-wave amplitude increased (Fig. 2-right). Again, the latter cannot be localised precisely in time, so an interval is specified. The pinch test was negative during the deep phase and positive during the shallow phase. The intervals within which the spectral amplitudes of δ- and θ-waves were calculated and the coupling asymmetry tested with surrogate data, before/after the transition from deep to light anæsthesia, are also provided. All values are in minutes.

Event	Time of event (minutes from start of anæsthesia) for each rat									
KX	1	2	3	4	5	6	7	8	9	10
Duration of recording	62	57	168	72	73	73	100	71	71	122
Increase in f_r	18	36	59	52	43	43	47	33	38	73
Decrease in the amplitude of δ	17±4	36±5	60±2	52±4	46±2	43±3	45±3	34±5	38±5	76±4
Interval before the transition	0-17	0-36	0-54	8-42	0-38	4-38	0-33	0-33	0-33	0-33
Interval after the transition	25-50	38-58	63-167	54-71	46-71	46-71	54-83	36-70	43-71	83-117
PB	1	2	3	4	5	6	7	8	9	10
Duration of recording	135	67	31	80	68	75	87	80	109	87
Increase in the amplitude of θ	60±3	16±4	2±1	20±3	14±5	30±5	27±5	28±4	30±4	35±3
Interval before the transition	0-55	0-10	-	0-15	-	0-25	0-20	0-24	0-35	0-30
Interval after the transition	65-135	20-67	5-31	25-80	12-68	35-75	35-87	35-80	35-109	40-87

Table 2: Cardiac and respiratory frequency data for the 20 rats. The intervals before and after the transition from deep to shallow anæsthesia, as specified in Table 1, are used to calculate average heart rate (f_c) and respiratory frequency (f_r) for each rat. All values are in Hz.

KX	1	2	3	4	5	6	7	8	9	10
f_c before	4.2	4.4	5.8	4.0	4.3	5.1	3.9	4.0	4.3	4.9
f_c after	4.3	4.2	5.3	3.7	3.7	4.7	3.6	5.2	6.2	6.5
f_r before	0.8	1.3	1.4	0.8	1.3	1.1	0.8	1.0	1.1	1.0
f_r after	1.8	1.9	1.9	0.8	2.1	3.1	1.4	2.7	3.0	1.9
PB	1	2	3	4	5	6	7	8	9	10
f_c before	5.7	5.3	6.3	6.8	6.4	6.1	5.5	5.9	4.9	5.3
f_c after	5.3	4.5	6.0	6.5	6.2	5.6	5.2	4.8	5.0	4.7
f_r before	1.0	0.7	2.2	1.0	1.2	0.8	0.8	1.0	0.8	0.7
f_r after	0.6	0.5	1.3	1.0	1.1	0.8	0.8	0.9	0.7	0.6

Table 3: Statistical tests of directional couplings. The couplings from cardiac to respiratory (C $\rightarrow$ R) and from respiratory to cardiac (R $\rightarrow$ C) activity are shown for both the KX and PB groups. The couplings from δ to respiratory ($\delta \rightarrow$ R), from respiratory to δ (R $\rightarrow \delta$), from δ to cardiac ($\delta \rightarrow$ C) and from cardiac to δ (C $\rightarrow \delta$) activity were calculated only for the KX group and only for the deep phase of anæsthesia. Each pair of numbers refers to measures before/after the deep/light anæsthesia transition. The times of the two intervals within which the directional coupling was calculated for each rat are specified in Table 1. The tests were performed as illustrated in Fig. 6. The "significance level" corresponds to the probability that the obtained CMI value occurred by chance, and was read from the cumulative histograms obtained by summing up the histogram bins from the estimated surrogate histograms such as those in Fig. 6. The result was considered significant for $p < 0.05$ (indicated by italicised numbers).

CMI	Significance level for each rat									
KX	1	2	3	4	5	6	7	8	9	10
C $\rightarrow$ R	*0.03*/0.45	0.23/*0.00*	0.14/0.90	0.14/0.60	0.80/0.90	0.90/*0.00*	0.80/*0.00*	0.20/0.90	0.20/0.10	0.70/0.90
R $\rightarrow$ C	*0.00*/0.70	*0.00*/0.90	0.34/0.70	*0.02*/0.60	*0.00*/*0.00*	*0.00*/0.07	0.10/0.40	*0.00*/0.70	*0.03*/0.50	*0.00*/0.50
$\delta \rightarrow$ R	0.50/-	0.25/-	0.33/-	0.70/-	0.08/-	0.40/-	*0.05*/-	0.50/-	0.07/-	0.22/-
R $\rightarrow \delta$	0.30/-	*0.03*/-	0.70/-	0.26/-	*0.02*/-	0.07/-	*0.03*/-	0.18/-	0.16/-	*0.05*/-
$\delta \rightarrow$ C	0.90/-	0.60/-	0.23/-	0.42/-	0.06/-	0.90/-	0.70/-	0.30/-	0.90/-	0.90/-
C $\rightarrow \delta$	0.10/-	0.90/-	0.90/-	0.64/-	0.60/-	0.50/-	0.26/-	0.90/-	0.90/-	0.50/-
PB	1	2	3	4	5	6	7	8	9	10
C $\rightarrow$ R	*0.00*/*0.04*	0.10/*0.00*	-/0.09	0.79/0.84	-/0.17	*0.02*/0.77	0.90/0.18	0.72/0.21	0.41/0.06	*0.04*/0.28
R $\rightarrow$ C	*0.00*/0.48	*0.00*/*0.00*	-/*0.00*	*0.00*/*0.00*	-/*0.00*	*0.00*/*0.00*	*0.00*/*0.00*	*0.00*/0.50	*0.00*/*0.00*	*0.00*/0.07

Figure captions

1. Extracts from the pre-processed time series: EEG (top panel); respiratory signal (middle); and ECG (bottom).

2. Evolution with time of the characteristic frequencies of EEG δ- and θ-oscillations during KX (left) and PB (right) anæsthesia, analysed by wavelet transform. For KX, two separate analyses using different frequency windows were needed to reveal the θ-activity, because of the dominance of the δ-waves. Note that the δ-oscillations occur only with KX and dramatically diminish at $\sim$40 minutes, which is when when the θ-oscillations emerge. The latter also appear for PB, almost simultaneously with positivity of the pinch-test; the sharp spectral peak near 1 Hz is spurious: it correponds to the respiratory frequency and results from movement artefacts due to respiration. Its second harmonic can also be seen.

3. Left: evolution with time of the EEG δ-wave f_δ (bottom), respiratory f_r (middle) and cardiac f_c (top) characteristic frequencies during KX anæsthesia. Right: evolution of f_r (bottom) and f_c (top) for PB. The dashed vertical lines indicate the separation of the two phases of anæsthesia in each case. The patterns of activity for both cardiac and respiratory frequencies differ substantially between the two groups. For the KX group, the phase of the f_δ wave could be detected reliably only during the deep phase of anæsthesia; for the PB group it could not be detected reliably in either phase.Left: evolution of the respiratory f_r (bottom), EEG δ-wave f_δ (middle) and cardiac f_c (top) characteristic frequencies with time during KX anæsthesia. Right: evolution of f_r (bottom) and f_c (top) for PB. The dashed vertical lines indicate the separation of the two phases of anæsthesia in each case. The patterns of activity for both cardiac and respiratory frequencies differ substantially between the two groups. For the KX group, the phase of the f_δ wave could be detected reliably only during the deep phase of anæsthesia; for the PB group it could not be detected reliably in either phase.

4. Direction of the cardio-respiratory interaction $d_{r,c}$ measured during (*a,b*) KX and (*c,d*) PB anæsthesia. (*a,c*) Calculated using the phase dynamics method (Rosenblum & Pikovsky 2001; Rosenblum *et al.* 2002). (*b,d*) Calculated from the same data using mutual information (Paluš *et al.* 2001*a*; Paluš & Stefanovska 2003). If $d_{r,c} > 0$ it means that respiration drives cardiac function, and *vice versa* if $d_{r,c} < 0$. The dashed lines separate the two phases of anæsthesia in each case.

5. Box plots presenting group median values and the distribution of wavelet amplitudes for deep and light anæsthesia within the δ (left) and θ (right) EEG frequency intervals for KX (top panels) and PB (bottom).

6. Use of surrogate data for testing the significance of the conditional mutual information (CMI) calculated from the data. The ordinates plot the relative frequencies with which the CMI surrogate realisation falls in a paricular histogram bin and are in dimensionless units. The CMI characterizes the information flow (influence) from respiratory to cardiac activity (a,c), and in the opposite direction from cardiac to respiratory activity (b,d), for a rat during KX anæsthesia. The top two panels (a,b) refer to a period 0–33 min. within the first part of the anæsthesia, and the lower panels (c,d) refer to a period 43–71 min. within the second part. CMI values calculated from the rat data under test are shown by the positions of the vertical bars; the distributions of 2500 realizations of surrogate data are shown by their histograms, obtained in each case using 100 bins.

7. Schematic diagram illustrating the main results of the study in terms of the 3-oscillator model of respiratory (r), cardiac (c) and cortical (δ) mutual interactions (arrows). Inter-oscillator interactions during (a,c) the period of deep anæsthesia are compared with those during (b,d) shallow anæsthesia with KX (a,b) and PB (c,d) respectively. The significances of the calculated CMIs (inter-oscillator couplings) are indicated by the numbers of stars (** for $N > 6$, * for $3 < N < 6$, and 0 for $N < 3$, where N is number of rats). A "?" is used to indicate cases where an interaction could not be evaluated (the phases of EEG δ-waves were difficult to detect unambiguously during shallow anaesthesia with KX), and throughout the entire period of PB anæsthesia).

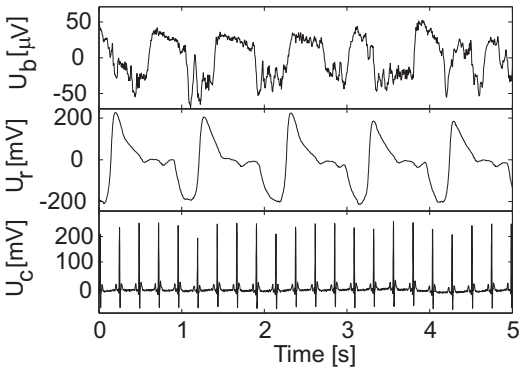

Figure 1: Extracts from the pre-processed time series: EEG (top panel); respiratory signal (middle); and ECG (bottom).

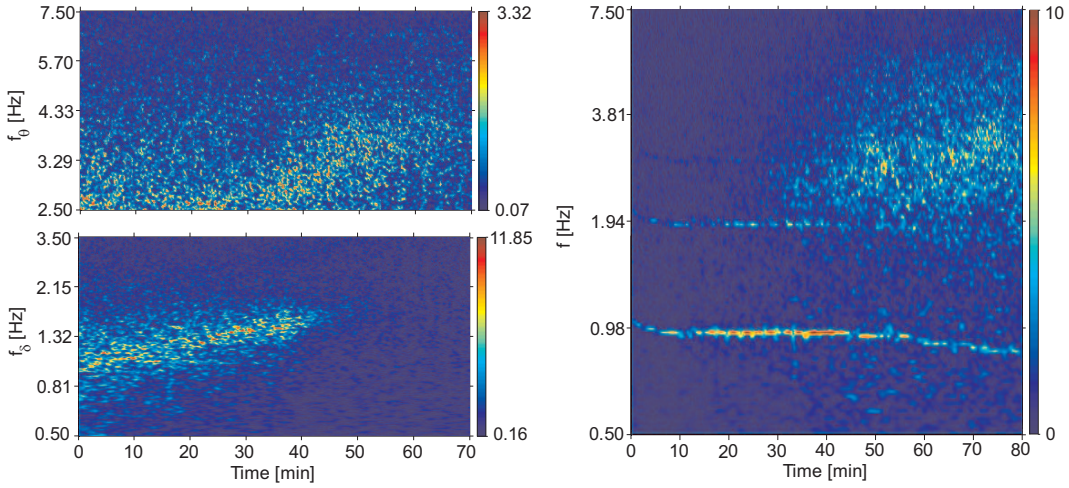

Figure 2: Evolution with time of the characteristic frequencies of EEG δ- and θ-oscillations during KX (left) and PB (right) anæsthesia, analysed by wavelet transform. For KX, two separate analyses using different frequency windows were needed to reveal the θ-activity, because of the dominance of the δ-waves. Note that the δ-oscillations occur only with KX and dramatically diminish at $\sim$40 minutes, which is when when the θ-oscillations emerge. The latter also appear for PB, almost simultaneously with positivity of the pinch-test; the sharp spectral peak near 1 Hz is spurious: it correponds to the respiratory frequency and results from movement artefacts due to respiration. Its second harmonic can also be seen.

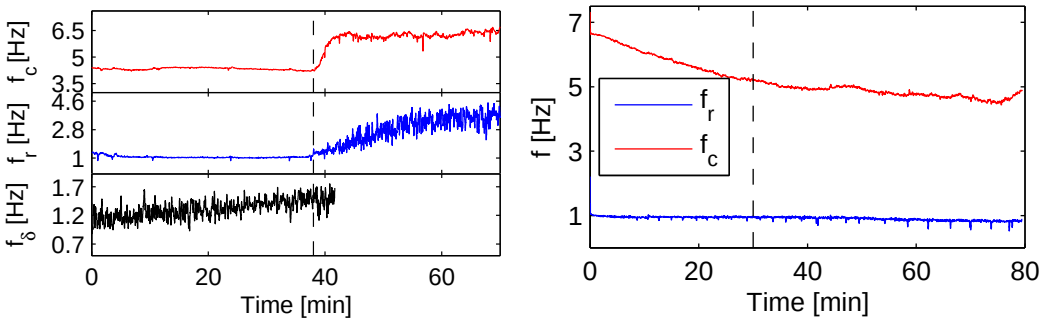

Figure 3: Left: evolution with time of the EEG δ-wave f_δ (bottom), respiratory f_r (middle) and cardiac f_c (top) characteristic frequencies during KX anæsthesia. Right: evolution of f_r (bottom) and f_c (top) for PB. The dashed vertical lines indicate the separation of the two phases of anæsthesia in each case. The patterns of activity for both cardiac and respiratory frequencies differ substantially between the two groups. For the KX group, the phase of the f_δ wave could be detected reliably only during the deep phase of anæsthesia; for the PB group it could not be detected reliably in either phase.

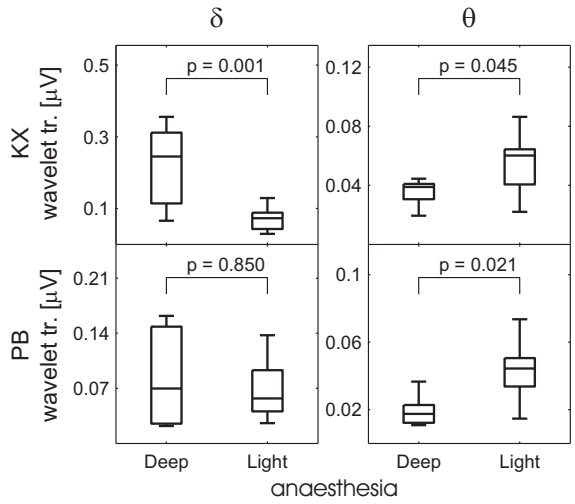

Figure 4: Box plots presenting group median values and the distribution of wavelet amplitudes for deep and light anæsthesia within the δ (left) and θ (right) EEG frequency intervals for KX (top panels) and PB (bottom).

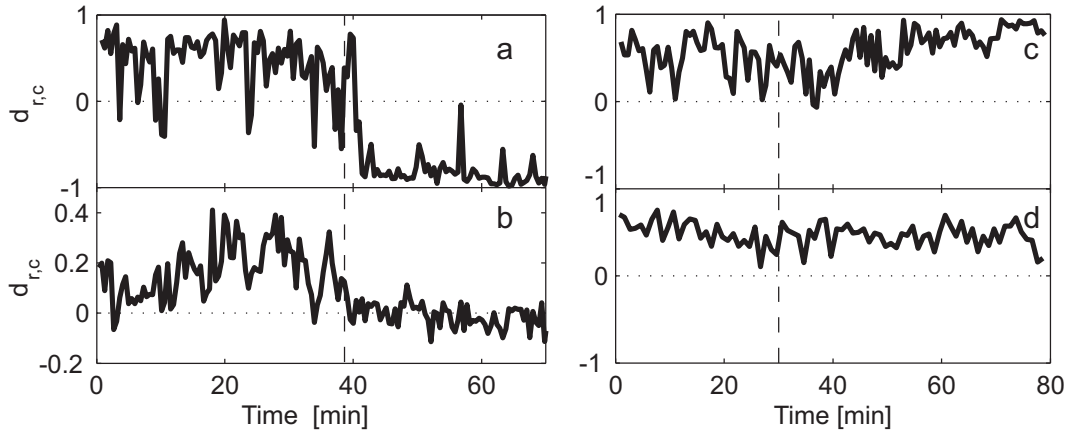

Figure 5: Direction of the cardio-respiratory interaction $d_{r,c}$ measured during (a,b) KX and (c,d) PB anæsthesia. (a,c) Calculated using the phase dynamics method (Rosenblum & Pikovsky 2001; Rosenblum *et al.* 2002). (b,d) Calculated from the same data using mutual information (Paluš *et al.* 2001*a*; Paluš & Stefanovska 2003). If $d_{r,c} > 0$ it means that respiration drives cardiac function, and *vice versa* if $d_{r,c} < 0$. The dashed lines separate the two phases of anæsthesia in each case.

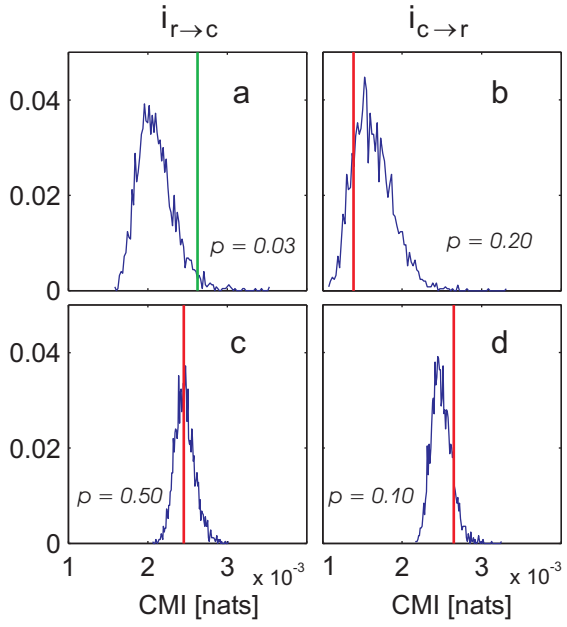

Figure 6: Use of surrogate data for testing the significance of the conditional mutual information (CMI) calculated from the data. The ordinates plot the relative frequencies with which the CMI surrogate realisation falls in a paricular histogram bin and are in dimensionless units. The CMI characterizes the information flow (influence) from respiratory to cardiac activity (a,c), and in the opposite direction from cardiac to respiratory activity (b,d), for a rat during KX anæsthesia. The top two panels (a,b) refer to a period 0–33 min. within the first part of the anæsthesia, and the lower panels (c,d) refer to a period 43–71 min. within the second part. CMI values calculated from the rat data under test are shown by the positions of the vertical bars; the distributions of 2500 realizations of surrogate data are shown by their histograms, obtained in each case using 100 bins.

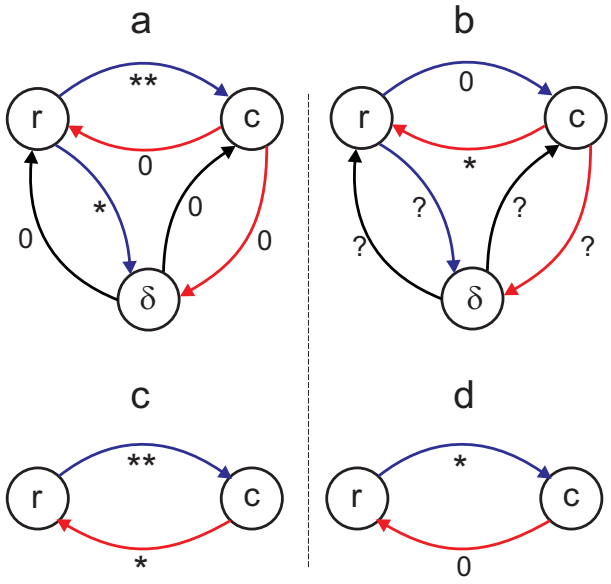

Figure 7: Schematic diagram illustrating the main results of the study in terms of the 3-oscillator model of respiratory (r), cardiac (c) and cortical (δ) mutual interactions (arrows). Inter-oscillator interactions during (a,c) the period of deep anæsthesia are compared with those during (b,d) shallow anæsthesia with KX (a,b) and PB (c,d) respectively. The significances of the calculated CMIs (inter-oscillator couplings) are indicated by the numbers of stars (** for $N > 6$, * for $3 < N < 6$, and 0 for $N < 3$, where N is number of rats). A "?" is used to indicate cases where an interaction could not be evaluated (the phases of EEG δ-waves were difficult to detect unambiguously during shallow anaesthesia with KX, and throughout the entire period of PB anæsthesia.